Sagisaka, M., Ono, S., James, C., Yoshizawa, A., Mohamed, A., Guittard, F., ... Eastoe, J. (2017). Anisotropic reversed micelles with fluorocarbon-hydrocarbon hybrid surfactants in supercritical CO_2. *Colloids and Surfaces B: Biointerfaces*. https://doi.org/10.1016/j.colsurfb.2017.12.012

Anisotropic reversed micelles with fluorocarbon-hydrocarbon hybrid surfactants in supercritical CO_2

Masanobu Sagisaka[a,], Shinji Ono[a], Craig James[a], Atsushi Yoshizawa[a], Azmi Mohamed[b,c], Frédéric Guittard[d], Robert M. Enick[e], Sarah E. Rogers[f], Adam Czajka[g], Christopher Hill[g], and Julian Eastoe[g,*]*

[a] Department of Frontier Materials Chemistry, Graduate School of Science and Technology, Hirosaki University, 3 Bunkyo-cho, Hirosaki, Aomori 036-8561, JAPAN

[b] Department of Chemistry, Faculty of Science and Mathematics, Universiti Pendidikan Sultan Idris, 35900 Tanjong Malim, Perak, Malaysia

[c] Nanotechnology Research Centre, Faculty of Science and Mathematics, Universiti Pendidikan Sultan Idris, 35900 Tanjong Malim, Perak, Malaysia

[d] Univ. Cote d'Azur, NICE-Lab, 61-63 av. S. Viel, 06200 Nice, France

[e] Department of Chemical and Petroleum Engineering, University of Pittsburgh, 940 Benedum Hall, 3700 O'Hara Street, Pittsburgh, Pennsylvania 15261, United States

[f] ISIS-CCLRC, Rutherford Appleton Laboratory, Chilton, Oxon OX11 0QX, U.K.

[g] School of Chemistry, University of Bristol, Cantock's Close, Bristol BS8 1TS, U.K.

*Corresponding authors

E-mail addresses: sagisaka@hirosaki-u.ac.jp (M. Sagisaka), Julian.Eastoe@bristol.ac.uk (J. Eastoe)

Abstract

Previous work (M. Sagisaka, et al. *Langmuir* 31 (2015) 7479-7487), showed the most effective fluorocarbon (FC) and hydrocarbon (HC) chain lengths in the hybrid surfactants FC*m*-HC*n* (sodium 1-oxo-1-[4-(perfluoroalkyl)phenyl]alkane-2-sulfonates, where *m* = FC length and *n* = HC length) were *m* and *n* = 6 and 4 for water solubilization, whereas *m* 6 and *n* 6, or *m* 6 and *n* 5, were optimal chain lengths for reversed micelle elongation in supercritical CO_2. To clarify why this difference of only a few methylene chain units is so effective at tuning the solubilizing power and reversed micelle morphology, nanostructures of water-in-CO_2 (W/CO_2) microemulsions were investigated by high-pressure small-angle neutron scattering (SANS) measurements at different water-to-surfactant molar ratios (W_0) and surfactant concentrations. By modelling SANS profiles with cylindrical and ellipsoidal form factors, the FC6-HC*n*/W/CO_2 microemulsions were found to increase in size with increasing W_0 and surfactant concentration. Ellipsoidal cross-sectional radii of the FC6-HC4/W/CO_2 microemulsion droplets increased linearly with W_0, and finally reached ~39 Å and ~78 Å at W_0 = 85 (close to the upper limit of solubilizing power). These systems appear to be the largest W/CO_2 microemulsion droplets ever reported. The aqueous domains of FC6-HC6 rod-like reversed micelles increased in size by 3.5 times on increasing surfactant concentration from 35 mM to 50 mM: at 35 mM, FC6-HC5 formed rod-like reversed micelles 5.3 times larger than FC6-HC6. Interestingly, these results suggest that hybrid HC-chains partition into the microemulsion aqueous cores with the sulfonate headgroups, or at the W/CO_2 interfaces, and so play important roles for tuning the W/CO_2 interfacial curvature. The super-efficient W/CO_2-type solubilizer FC6-HC4, and the rod-like reversed micelle forming surfactant FC6-HC5, represent the most successful cases of low fluorine content additives. These surfactants facilitate VOC-free, effective and energy-saving CO_2 solvent systems for applications such as extraction, dyeing, dry cleaning, metal-plating, enhanced oil recovery and organic/inorganic or nanomaterial synthesis.

Graphical abstract

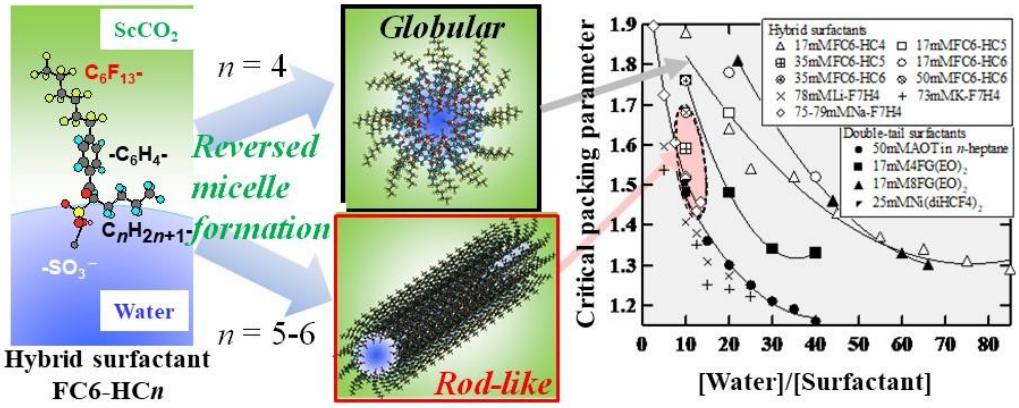

Highlights

- Anionic hybrid surfactants, FC6-HC*n*, were studied in supercritical CO_2 (sc-CO_2).
- FC6-HC5 having alkyl length (*n*) of 5 formed rod-like water-in-CO_2 (W/CO_2) microemulsion droplets.
- FC6-HC4 generated the largest globular W/CO_2 microemulsion droplets reported to date.
- FC6-HC5 was identified as the best surfactant for increasing sc-CO_2 viscosity.
- The CO_2- and hydrophobic alkyl chains play important roles for tuning W/CO_2 curvature.

Keywords

Supercritical CO_2, Microemulsion, Hybrid surfactant, Solubilizing power, Small-Angle Neutron Scattering

1. Introduction

Supercritical CO_2 ($scCO_2$) has received much attention for its use in industrial applications owing to attractive properties such as low cost, inflammability, natural abundance, high mass transfer, and pressure/temperature-tunable solvency (or CO_2 density) [1]. As such, $scCO_2$ is currently used in numerous applications including as a green solvent for organic synthesis, dry cleaning, polymerization, extraction, nanomaterial processing, and enhanced oil recovery (EOR). Unfortunately, supercritical CO_2 can only effectively dissolve nonpolar and small molecular mass materials [2]. The low viscosity of CO_2 is usually a desirable attribute that leads to increased mass transfer. However, a significant problem when using $scCO_2$ during enhanced oil recovery (EOR)is that the CO_2 viscosity is significantly lower than that of the oil being displaced, leading to inefficient volumetric sweep of the porous media [3]. Improving the poor solubility of polar materials and increasing the viscosity for EOR are both important aims for developing potential applications of $scCO_2$. One of the most promising approaches to overcoming these limitations of sc-CO_2 is to generate reversed micelles with high-polarity aqueous cores in the continuous $scCO_2$ phase (i.e. water-in-$scCO_2$ microemulsions, W/CO_2 µEs) [2-3]. Such multi-component self-assembly systems display not only the attractive characteristics of $scCO_2$, but also the solvation properties of bulk water, and so they have potential as volatile organic compound (VOC)-free and energy-efficient solvents for nano-material synthesis, enzymatic reactions, dry-cleaning, dyeing, and preparation of inorganic/organic hybrid materials [2]. Additionally, if reversed micelles can be formed with rod-like morphologies, they can also effectively enhance the $scCO_2$ viscosity [3]. To be a viable green and economical technology, the amount of surfactant used for W/CO_2 µEs should be as small as possible. This minimal surfactant concentration does however have to be balanced against the need for the large interfacial areas required to form W/CO_2 µEs, and the appropriate levels of dispersed water needed to enhance process efficiencies. Clearly, it is of interest to develop highly efficient surfactants for W/CO_2 µEs and formation of rod-like reversed micelles, and field has been actively researched since the early 1990s [4].

The development of CO_2-philic hydrocarbon surfactants for $scCO_2$ has been recognized as an important task for economic and environmental reasons [4-8]. Studies into CO_2-philic materials have been

performed on commercially available polymers, surfactants, and other oleo-philic substances. However, those commercial compounds were basically insoluble in $scCO_2$ and therefore inappropriate for modifying $scCO_2$ properties [4]. Even the common commercial surfactant Aerosol-OT (sodium bis-(2-ethyl-1-hexyl) sulfosuccinate, AOT), which is widely used for water-in-oil (W/O) microemulsion formulation, is inactive in $scCO_2$ and hence ineffective at stabilizing W/CO_2 µEs [4]. After initial studies it became apparent that conventional surfactant-design theory cannot be applied to W/CO_2 systems, and that CO_2-philicity is not directly comparable to oleo-philicity. Therefore, the creation of CO_2-philic surfactants has required new directions and paradigms in the field of surfactant molecular-design. Based on new design principles, tailor-made surfactants able to stabilize W/CO_2 µEs, and generate rod-like reversed micelles in $scCO_2$ have been made [3].

Currently, the use of highly branched hydrocarbon chains, especially containing methyl-branches, ester and ether groups, has been reported to increase surfactant solubility in $scCO_2$ [5-8]. Unfortunately, an efficient and cost-effective hydrocarbon stabiliser for W/CO_2 µEs, (like AOT commonly used for W/O µEs [9]) has not yet been found.

Many earlier studies reported that certain fluorinated surfactants, including perfluoropolyethers (PFPFs) and fluorinated AOT analogues, could dissolve in CO_2 and exhibit a high W/CO2 interfacial activity, hence suggesting the feasibility of forming W/CO_2 µEs [10-13]. The water-solubilizing power in CO_2 was often discussed in terms of the water-to-surfactant molar ratio W_0 (=[water]/[surfactant]). Hereafter, the maximal W_0 achievable in a single-phase W/CO_2 µE, namely W_0^{max}, is used to evaluate the solubilizing power. Typical benchmark values for PFPE surfactants are W_0^{max} up to ~20 [10-13].

It is not yet fully understood why fluorocarbon surfactants are so effective at stabilizing W/CO_2 µEs, however, recent molecular simulation studies [14,15] have indicated that as compared with HC chains, FC groups have (1), stronger interactions with CO_2 via quadrupolar and dispersion interactions, and (2), weaker FC-FC chain-chain interactions due to a weak repulsion, being electrostatic in origin. These properties conspire together to so that reversed micelles of FC surfactants achieve better solvation by CO_2, and this, in turn, causes lower surfactant interfacial packing densities and weaker attractive inter-

micellar interactions compared with hydrocarbon surfactant analogues. However, despite these attractive properties, due to high fluorine content these F-surfactants bring disadvantages of cost and biocompatibility, thus preventing their use in applications [16]. Therefore, there is quest for CO_2-philic surfactants with as low fluorination as possible.

Other investigations [17-20] introduced a class of fluorinated AOT analogues yielding W/CO_2 µEs with $W_0 \leq 30$ (e.g. sodium bis(1*H*,1*H*,5*H*-octafluoropentyl)-2-sulfosuccinate, di-HCF4). Surfactants of di-HCF4 having Co^{2+} and Ni^{2+} counter ions, Co(di-HCF4)$_2$ and Ni(di-HCF4)$_2$, were reported to form rod-like reversed micelles, although di-HCF4 with Na^+ counterions formed only globular microemulsion droplets [21,22]. This suggests exchanging monovalent counterions for divalent cations can result in viscosity-enhancing rod-like reversed micelles. In addition, double-FC-tail phosphate surfactants were also found to be efficient µE stabilisers, the most favourable case stabilizing W_0 up to 45 [23-24].

Recently, with the aim of optimizing the surfactant structure of fluorinated AOT analogues for W/CO_2 µEs, double-FC-tail anionic surfactants with various FC lengths, and either sulfoglutarate or sulfosuccinate headgroups, were examined [25-29]. This allowed for the effect of not only FC length, but also the addition of a methylene spacers between the double tails to be explored. This work found that the solubilizing power of the glutarates *n*FG(EO)$_2$ to be generally higher than for the succinate analogues *n*FS(EO)$_2$. The most efficient surfactant was found to be 4FG(EO)$_2$ which, despite having the shortest FC (perfluorobutyl) tails, could stabilize microemulsions of W_0^{max} = 80 at 75°C [25]. Considering that fluorocarbons are CO_2-philic groups and longer FC surfactants generally have higher solubilizing power [25-29], the fact that this high stability can be obtained with only the shortest chain FC 4FG(EO)$_2$ is at first sight surprising. In further studies, the minimum fluorine content necessary to render a surfactant CO_2-philic has been identified by using double-pentyl-tail surfactants with different fluorination levels [30,31]. In these surfactants, at least two fluorinated carbons (CF_3CF_2-) were required to stabilise W/CO_2 µEs. Through these studies, the understanding behind the effect of FC-tail length on W/CO_2 µEs stabilization and solubilizing power and for symmetrical double FC-tail surfactants (i.e. fluorinated AOT-analogues) is improving.

As for the fully fluorinated surfactant series, two-tail hybrid surfactants, having separate HC and FC chains in the same molecule, have also been evaluated for stabilization of W/CO_2 µEs. The first successful example of a CO_2-philic hybrid surfactant was sodium 1-pentadecafluoroheptyl-1-octanesulfate (F7H7, $(C_7H_{15})(C_7F_{15})CHOSO_3Na$), which solubilized water up to W_0^{max} = 35 [32]. Further studies [3,33,34] of hybrid surfactants related to F7H7 but with different FC and HC chain lengths, M-F*m*H4 (Counter ion M= Li, Na, and K, fluorocarbon length *m* = 7 and 8), observed the formation of W/CO_2 µEs for most of the analogues, but with smaller attainable W_0^{max} values than for F7H7. On the other hand, these hybrid surfactant systems were often reported to form elongated reversed micelles [3,33,34], whereas those formed by regular non-hybrid surfactants were likely to be spherical. The formation of elongated aggregates with a high aspect ratio (rod length/diameter) can serve to thicken dense CO_2, and appears to be a viable way to achieve higher efficiencies in EOR applications [3]. Unfortunately, these unique characteristics have never been examined in detail in terms of the hybrid tail structure (e.g. effect of FC and HC length and the balance of both).

Recently, a series of hybrid surfactants, sodium 1-oxo-1-[4-(perfluoroalkyl)phenyl]alkane-2-sulfonates, FC*m*-HC*n* (FC length *m* = 4, 6, HC length *n* = 2, 4, 5, 6 and 8) were used to clarify the effects of FC and HC chain length on the phase stability and nanostructures of the reversed micelles formed [26,35]. The optimal HC-tail and FC-tail length in this hybrid surfactant was found to be *n* = 4 and *m* 6 respectively (i.e. FC6-HC4). This surfactant was able to yield µEs with a maximum solubilizing power, W_0^{max} of 80; a value equal to the highest performance yet reported in W/CO_2 systems [3-35]. The identification of an optimal HC-length is very interesting, since straight-chain HCs were commonly considered not to be CO_2-philic [4] and their inclusion in FC-surfactant molecules was intentionally limited in order to retain CO_2-philicity. To evaluate the effectiveness per F-atom the solubilizing power per F-atom was estimated as 6.2/F atom, which is ~1.5 times larger than the most effective FC-surfactant found in earlier papers [10-35]. The highest effectiveness per F-atom generated by hybrid structures is also an interesting concept design of new CO_2-philic surfactants. High pressure-small angle neutron scattering (HP-SANS) measurements [35] was used to size the D_2O cores of FC6-HC*n* reversed micelles

at W_0 = 20, and gave evidence for shape transitions in core morphology after increasing HC-tail length (ellipsoid for n = 4 → cylinder for n = 5 and 6 → sphere for n = 8). The micelle shape-anisotropy and aspect ratio were seen to reach a maximum of 6.3 at a HC-tail length n = 6.

How does a hybrid surfactant stabilise W/CO_2 µEs and also form elongated reversed micelles? What is the role of the non-CO_2-philic HC-tails? Although these questions have not yet been clarified, they remain interesting and important topics for chemists in this field. To improve understanding about CO_2-philic surfactant design, this study has focused on the effect of the hybrid tail structure (e.g. FC-HC balance) on solubilizing power, micellar aggregate size and shape in scCO_2. This provides important information on structure-property relationships for hybrid surfactants such as hydrophilic/CO_2-philic balance (HCB) [36], critical packing parameter (CPP) [37], interactions between tail-tail and tail-head groups [38]. This is an important step in obtaining optimized, super-efficient, low fluorine content surfactants for applications of W/CO_2 µEs and CO_2-based fluids in general.

With the aim of clarifying the role of the HC-tail in hybrid surfactants, this study has examined reversed micelle nanostructures and molecular properties (i.e. CPP an area per molecule) of FC6-HC*n* in water/supercritical CO_2 mixtures using HP-SANS measurements and detailed SANS data analyses. The findings described here suggest new directions and strategies for developing CO_2–philic surfactants for stabilizing µEs and elongated reversed micelles, both of which are applicable to many practical applications.

2. Experimental Section

2.1. Materials

The family of surfactants studied here are hybrid surfactant sodium 1-oxo-1-[4-(perfluoroalkyl)phenyl]alkane-2-sulfonates, FC*m*-HC*n* (FC length *m* = 6, HC length *n* = 4, 5, 6 and 8). The surfactants FC*m*-HC*n* with *m*/*n* = 6/6, and 6/8 were provided by Prof. Yoshino and Dr. Kondo at Tokyo University of Science [39]. The other surfactants FC6-HC4 and FC6-HC5 were synthesised and purified as described in the reference [35].

Structures of FC*m*-HC*n* and the other control hybrid surfactants F*m*H*n* are shown in **Table 1** along with the interfacial properties of aqueous solutions obtained by standard measurements [3,33-35,40,41]. Ultrapure water with a resistivity of 18.2 MΩ cm was obtained from a Millipore Milli-Q Plus system. CO_2 was of > 99.995% purity (Taiyo Nippon Sanso Corp.). The structures of the steric models and the length of surfactant molecules (in isolation) were calculated by MM2 (Molecular Mechanics program 2) calculations (Chem 3D; CambridgeSoft Corp., Cambridge, MA).

Table 1 Interfacial properties of hybrid surfactants FC*n*-HC*m* and F*m*H*n* in water at 25 ºC.

Main structure	Surfactant	R_1 / R_2	T_K [a] / ºC	CMC [b] / M	γ_{CMC} [c] /(mN m^{-1})	$A_{A/W}$ [d] / Å^2
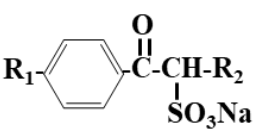	FC6-HC4	$F(CF_2)_6$- / $H(CH_2)_4$-	15	2.3×10^{-4}	20.4	105
	FC6-HC5	$F(CF_2)_6$- / $H(CH_2)_5$-	10	1.3×10^{-4} [e]	18.0 [e]	72 [e]
	FC6-HC6	$F(CF_2)_6$- / $H(CH_2)_6$-	48	5.5×10^{-5} [f]	16.2 [f]	98 [f]
	FC6-HC8	$F(CF_2)_6$- / $H(CH_2)_8$-	> 95	—	—	—
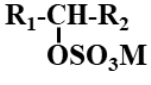	Li-F7H4 (M=Li)	$F(CF_2)_7$- / $H(CH_2)_4$-		2.2×10^{-3}	26.0	106
	K-F7H4 (M=K)	$F(CF_2)_7$- / $H(CH_2)_4$-		1.4×10^{-3}	22.1	62
	Na-F7H4 (M=Na)	$F(CF_2)_7$- / $H(CH_2)_4$-		1.9×10^{-3}	23.8	67
	Na-F8H4 (M=Na)	$F(CF_2)_8$- / $H(CH_2)_4$-		7.8×10^{-4}	25.4	68

[a] Krafft temperature, [b] Critical micelle concentration in water. [c] Surface tension at CMC. [d] Molecular area at CMC obtained by using the Gibbs adsorption equation. The uncertainties of $A_{A/W}$ are ±5 Å^2. [e] at 35 ºC. [f] at 50 ºC.

2.2 High-Pressure Small-Angle Neutron Scattering (HP-SANS) measurements and data analysis

Due to the range of neutron wavelengths available, time-of-flight SANS is suitable for studying the shapes and sizes of colloidal systems. High-pressure SANS (HP-SANS) is a particularly important technique for determining aggregate nanostructure in supercritical CO_2. The HP-SANS measurements of the D_2O/hybrid compound/scCO_2 systems were performed at 45 °C at various pressures. The LOQ and the SANS2D time-of-flight instruments, at the Rutherford Appleton Laboratory at ISIS UK, were used in conjunction with a stirred, high-pressure cell (Thar). The path length in the cell and neutron beam diameter were both 10 mm. The measurements gave absolute scattering cross sections $I(Q)$ (cm^{-1}) as a function of momentum transfer Q ($Å^{-1}$), which is defined as $Q = (4\pi/\lambda)\sin(\theta/2)$, where θ is the scattering angle. The accessible Q ranges were 0.007-0.22 $Å^{-1}$ for LOQ and 0.002-1.0 $Å^{-1}$ for SANS2D arising from an incident neutron wavelength, λ, of 2.2-10 Å. The data were normalised for transmission, empty cell, solvent background, and pressure induced changes in cell volume as before [19-23,29-31,33-35].

Pre-determined amounts of D_2O and surfactant, where the molar ratios of surfactant to CO_2 were fixed at 8.0×10^{-4}, 1.7×10^{-3} and 2.4×10^{-3} (= 17, 35 and 50 mM at the appropriate experimental condition, respectively), were loaded into the Thar cell. Then, CO_2 (11.3g), was introduced into the cell by using a high pressure pump, and the surfactant/D_2O/CO_2 mixture was pressurised to 350 bar at 45 ºC by decreasing the inner volume of the Thar cell. With vigorous stirring, visual observation was carried out to identify if any mixture was either a transparent single-phase (W/CO_2 µE), or a turbid phase-separate system. Finally, the HP-SANS experiments were performed for not only single-phase W/CO_2µEs, but also the turbid phases formed below the cloud point phase transition pressure P_{trans}. Due to the systems being dilute dispersions (volume fractions typically 0.05 or less), the physical properties of the continuous phase of scCO_2 were assumed to be equivalent to those of pure CO_2.

Scattering length densities of surfactants, CO_2 and D_2O were calculated as in supplementary data (See section S1). The shells of FC6-HC*n*/D_2O/CO_2 µEs were estimated to be composed of the perfluorohexyl-phenylene groups, and the scattering length density, ρ_{shell}, was calculated as 2.69×10^{10}

cm^{-2} from equation (S1) in supplementary data. The average mass densities values of benzene and perfluorohexane at 25 ˚C were 0.88 g and 1.67 g cm^{-3} respectively [42]. As ρ_{shell} was close to ρ_{CO2} (2.29 $\times 10^{10}$ cm^{-2}) and the shells are solvated with CO_2 to get both scattering length densities closer, neutron scattering from the shells was identified to be negligible. Therefore SANS from the D_2O/CO_2 µEs was assumed to only be from the so-called aqueous core contrast.

For model fitting data analysis, the W/CO_2 µE droplets were treated as cylindrical or ellipsoidal particles with a Schultz distribution in core radius and length [43]. The polydispersities in ellipsoid and cylinder radii and cylinder length were fixed at 0.3 as found in spherical D_2O/CO_2 µEs with the double FC-tail surfactants (polydispersity = 0.17-0.40) [29, 35, 44]. Full accounts of the scattering laws are given elsewhere [43, 44].

Data have been fitted to the models described above using the SasView small-angle scattering analysis software package (http://www.sasview.org/). The fitted parameters are the core radii perpendicular to the rotation axis ($R_{f\text{-}ell,a}$) and along the rotation axis ($R_{f\text{-}ell,b}$) for ellipsoidal particles, or the core radius R_{cyl} and the length L_{cyl} for cylindrical particles; these values were initially obtained by preliminary Guinier analyses ($L_{g\text{-}disk}$, $R_{g\text{-}disk}$, and $R_{g\text{-}sph}$) [29,35,44,45].

3. Results and Discussion

3.1 Growth and morphology changes for FC6-HC*n*/W/CO_2 µEs with loading water

To examine changes in the shape and size of D_2O/CO_2 µEs with FC6-HC4 and FC6-HC6 as a function of W_0, SANS $I(Q)$ profiles with different W_0 values were measured at a constant surfactant concentration of 16.7 mM at 45 ºC and 350 bar. SANS data along with the fitted $I(Q)$ functions are shown in **Figure 1**.

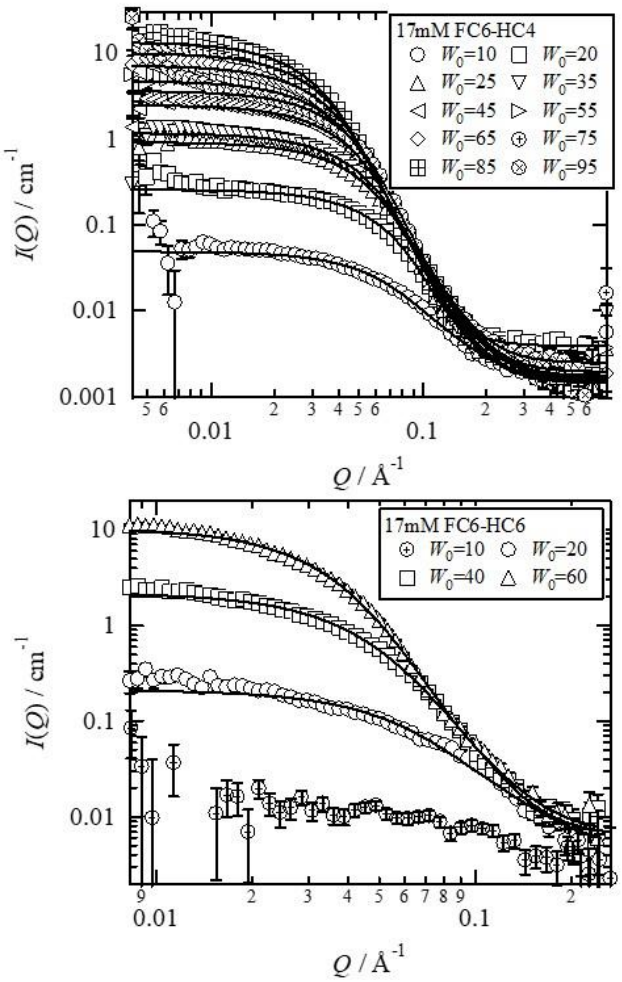

Figure 1. SANS profiles for FC6-HC*n* (*n* = 4 or 6)/D_2O/CO_2 mixtures with different W_0 values at 45 ºC and 350 bar (CO_2 density = 0.92 g/cm^3). Fitted curves were based on a model incorporating a Schultz distribution of polydisperse ellipsoid particles. The molar ratio of the surfactant to CO_2 was fixed at 8×10^{-4} ([Surfactant] = ~16.7 mM at the experimental conditions).

SANS profiles are useful in determining the shape of nano- and colloidal particles. With W_0 values lower than their maximum solubilizing powers (W_0^{max} = 80 for FC6-HC4 and 55 for FC6-HC6 under the experimental conditions [35]), FC6-HC4 and FC6-HC6 exhibited transparent single-phases giving distinct SANS profiles. Although turbid phases appeared as W_0 exceeds W_0^{max}, a SANS curve from D_2O droplets was still observed. In the low Q region for FC6-HC4, the scattering intensity increased with W_0 until W_0 = 85, suggesting growth of the µE droplets with increased water loading. The analysis of SANS profiles clearly demonstrated the highest solubilizing power W_0^{max} = 80 of FC6-HC4 in surfactant/$scCO_2$ systems ever reported.

In the low Q region (typically in the case of droplet µEs < 0.01 $Å^{-1}$), the scattering may scale as $I(Q) \sim Q^{-D}$, where D is a characteristic "fractal dimension" for the colloids; hence, the gradient of a log-log plot will be $-D$. In the case of non-interacting spheres, D should be zero in this low Q region, whereas D = 1 for cylinders and 2 for disks [29, 35, 44, 45]. The SANS profiles for FC6-HC4 and FC6-HC6 at 16.7mM show D = 0 and 1, suggesting the presence of globular or rod-like nanodomains, respectively. Methods exist to approximate radius from SANS data for globular µEs using Guinier plots [29, 35, 44, 45] (Ln [$I(Q)$] vs Q^2) and Porod plots ($I(Q)\ Q^4$ vs Q) as shown in supplementary data (**Figures S1** and **S2**). Radii of gyration (R_g) and sphere radius ($R_{g\text{-}sph}$) from Guinier plots and sphere radius (R_{prd}) from Porod plots are presented in **Table S1** in supplementary data. The radii R_g and R_{prd} were similar at same W_0, lending confidence to these analyses.

The values of R_{prd} or R_g were employed as the starting points for model fit analyses using the full polydisperse Schultz ellipsoid or cylinder models. The parameter outputs are the average values of radii for the ellipsoidal D_2O cores ($R_{ell,a}$ and $R_{ell,b}$) or, where used, the radius and length of the cylindrical core (R_{cyl} and L_{cyl}). The polydispersity width was set at 0.3, which is a typical value for W/CO_2 µE systems (e.g. 0.17-0.40 for double FC-tail sulfonate surfactants [29,35,44]). These fitted parameters are also listed in **Table S1**.

When increasing W_0 from 25 to 95, for FC6-HC4, the ellipsoid radii gradually increased but the aspect ratios ($R_{ell\text{-}b}$ / $R_{ell\text{-}a}$) of the D_2O core was lower than two and comparable between samples. This

suggests a more globular, rather than elongated shape. However, this globular shape µE transformed into rod-like on decreasing the W_0 value to 10, or by increasing the HC-tail length from 4 to 6 to with surfactant FC6-HC6. This is reflected in the SANS data which for FC6-HC4 at W_0 = 10, and FC6-HC6 at W_0 = 20 were both well fitted using the cylindrical form factor model rather than the ellipsoidal one.

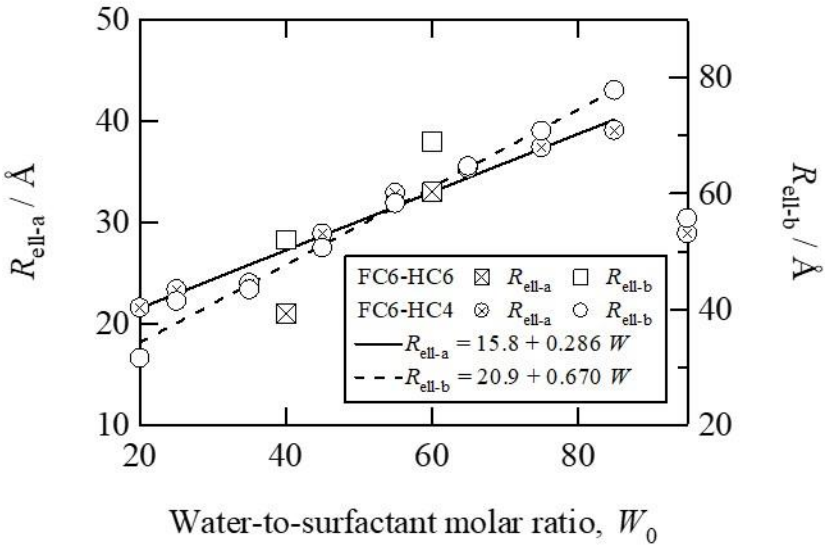

Figure 2. Changes in ellipsoidal aqueous core radii R_{ell-a} and R_{ell-b} for the 16.7 mM FC6-HC*n*/D_2O/CO_2 µEs as a function of W_0 at 45 ºC and 350 bar. The data were taken from **Table S1**. Solid and broken lines show linear functions fitted with the data for FC6-HC4 and FC6-HC6, respectively.

To clarify the growth of µE droplets with loading water, changes in radii R_{ell-a} and R_{ell-b} of the ellipsoid D_2O cores were plotted as a function of W_0 in **Figure 2**. In the case of the FC6-HC4/W/CO_2 µE, both radii increased with W_0 linearly; R_{ell-a} = 15.8 + 0.286 W_0 and R_{ell-b} =20.9 + 0.670 W_0. Eventually, R_{ell-a} and R_{ell-b} reached 39.1 Å and 77.8 Å at W_0 = 85 (≈ the maximum solubilizing power), identified as the largest core radius ever reported in a W/CO_2 µE systems [10-35]. Previous SANS studies dealing with double FC-tail surfactants *n*FG(EO)$_2$ with differing FC lengths (*n* = 4-8) found a linear relationship between spherical D_2O core radius, R_c, and W_0 where $R_c = \boldsymbol{a} + \boldsymbol{b}\ W_0$, where the constants $\boldsymbol{a}$ = 5.0-5.4 and $\boldsymbol{b}$ = 0.60-0.64 [29]. When comparing the average values of the constants, <*a*> and <*b*> found for

nFG(EO)$_2$ to the values found here for FC6-HC4 (<a> = 18.4, <b> = 0.478), <$\boldsymbol{b}$> for FC6-HC4 was slightly smaller than $\boldsymbol{b}$ for nFG(EO)$_2$ but the <$\boldsymbol{a}$> value was approximately 3.6 times larger than the $\boldsymbol{a}$ value. The constants $\boldsymbol{a}$ and $\boldsymbol{b}$ are known to strongly depend on volume of surfactant headgroup (v_{head}) and area per surfactant molecule (A), respectively, as shown in the relationship

$$\alpha(p)\, R_{\mathrm{c}} = (3v_{\mathrm{head}}/A) + (3v_{\mathrm{w}}/A)\, W_0 \quad (1)$$

where $\alpha(p) = 1 + 2p^2$, p is polydispersity index (σ/R_{c}), R_{c} is core radius, and v_{w} is volume of a water molecule [29,47]. Namely, the larger <$\boldsymbol{a}$> and the smaller <$\boldsymbol{b}$> values suggests FC6-HC4 to have a larger v_{head} and a smaller A than each value of nFG(EO)$_2$. Based on equation (3), volume-to-surface area ratio per aqueous core in reversed-type µE ($v_{\mathrm{core}}/s_{\mathrm{core}}$) can be expressed as,

$$\alpha(p)\, (v_{\mathrm{core}}/s_{\mathrm{core}}) = (v_{\mathrm{head}}\, N_{\mathrm{agg}} + v_{\mathrm{w}}\, W_0\, N_{\mathrm{agg}}) / (A\, N_{\mathrm{agg}}) = (v_{\mathrm{head}}/A) + (v_{\mathrm{w}}/A)\, W_0 \quad (2)$$

where N_{agg} is aggregation number. One advantage of using equation (2) is that is can be applied to a wide range of morphologies (spheres, ellipsoids, rods etc) whereas equation (1) is just for spherical reversed-type µEs. For detailed examination of v_{head} and A for FC6-HCn, ($v_{\mathrm{core}}/s_{\mathrm{core}}$) values calculated from $R_{\mathrm{ell\text{-}a}}$ and $R_{\mathrm{ell\text{-}b}}$ were plotted as a function of W_0, and displayed in **Figure 3**.

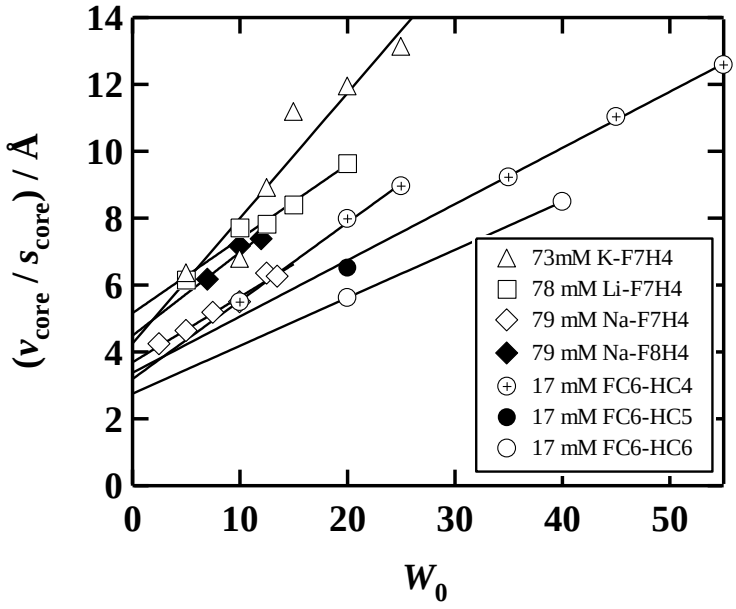

Figure 3. Relationship between volume-to-surface area ratio (v_{core}/s_{core}) of aqueous cores and W_0 for the 17mM FC6-HC$_n$/D$_2$O/CO$_2$ μEs at 45 ºC and 350 bar. The v_{core}/s_{core} values were calculated with ellipsoidal core radii listed in **Table S1**. The graph also displays data for D$_2$O/CO$_2$ μEs with 73 mM K-F7H4, 78 mM Li-F7H4, 75-79 mM Na-F7H4, 79 mM Na-F8H4 at 23-40 ºC and 380-400 bar reported in earlier papers [3,33,34].

Figure 3 also includes data for hybrid surfactants FC6-HC5, and M-F*n*H4 (CF$_3$(CF$_2$)$_m$-CH(-OSO$_3$M)-(CH$_2$)$_3$CH$_3$, m = 7 or 8, M = K, Li, or Na) reported in earlier papers [3,33,34]. Most (v_{core}/s_{core}) data in **Fig 3** could be expressed as linear functions, suggesting v_{head} and A can be calculated using equation (2). **Table 2** lists the values for area per surfactant molecule ($A_{v/s}$), v_{head}, and radius of headgroup (R_{head} = $(3v_{head} / 4\pi)^{1/3}$) as obtained from the slopes and intercepts in **Fig. 3**.

Table 2 Area per surfactant molecule ($A_{v/s}$), volume (v_{head}) and radius (r_{head}) of surfactant headgroup at W/CO_2 interface.

Surfactant	Conc. / mM	W_0	$A_{v/s}$ / Å^2	v_{head} / Å^3	r_{head} / Å
FC6-HC4*1	17	10-25	109	410	4.6
		35-55	152	600	5.2
FC6-HC6*1	17	20-40	177	580	5.2
K-F7H4*2	73	5-25	68	340	4.3
Li-F7H4*2	78	5-20	115	700	5.5
Na-F7H4*2	79	7-12	130	570	5.1
Na-F8H4*2	79	2.5-13.5	102	540	5.1

$A_{V/S}$ is area per surfactant headgroup obtained from the slopes, and v_{head} and r_{head} are volume and radius (if sphere model used) of headgroup from the intercepts in **Fig. 3**. The uncertainties of $A_{v/s}$, v_{head}, and r_{head} are ± 10 Å, ± 30 Å^3, and ± 0.3 Å. *1 at 45 ºC and 350 bar, *2 at 30 ºC and 500 bar

In the case of FC6-HC4, there are two linear functions describing the data; one for samples with W_0 values between 10 and 25 and one for W_0 values between 35 and 55. Both $A_{v/s}$ and v_{head} for data in the high W_0 region are larger by 1.4-1.5 when compared to data in the low W_0 region. This increase in area per surfactant molecule with W_0 was also found in A_{prd} values obtained from Porod analysis [46] (**Table S1, Figure S2**) and in earlier W/CO_2 µE studies [29, 44]. The trend most likely points to the swelling behaviour of the headgroup with water and counter-ion dissociation. When comparing between FC6-HC4 and FC6-HC6, $A_{v/s}$ for FC6-HC6 was larger at W_0 =35-55 in spite of the similar v_{head} and r_{head} values. The structural difference between both surfactants is just an ethylene unit in the HC-tail. Therefore, the increased $A_{v/s}$ results not from the headgroup but the increased bulkiness of the hydrophobic tail. As suggested in earlier studies [35, 47], this implies that when absorbed at the water interface, the HC-tails of the FC6-HC*n* are oriented toward the lateral direction (see **Figure S3** in supplementary data).

M-F*m*H4 are a series of hybrid surfactants having a slightly longer FC-chain, with a sulphate headgroup and no aromatic ring. When comparing FC6-HC4 and Na-F7H4 (which have similar structures) $A_{v/s}$ and v_{head} (or r_{head}) for FC6-HC4 at $W_0 \leq 25$ are lower than those of Na-F7H4, resulting from the smaller sulfonate headgroup of FC6-HC4. Counterion effects can also be found in the values of v_{head} (or r_{head}) in M-F7H4 surfactants with K^+, Na^+, and Li^+. The v_{head} (or r_{head}) value increases in the order of $Li^+ > Na^+ > K^+$. The order is likely to relate to the Hofmeister series [48], or degree of counterion dissociation of the sulfate group, that is $Li^+ > Na^+ > K^+$.

3.2 Elongation of FC6-HC*n* reversed micelles with increasing surfactant concentration

Earlier studies of W/CO_2 µEs found that with fluorinated surfactants, rod-like reversed micelles often form at low W_0 values of ~10 [3,21,22,33-35]. Previous SANS studies [35] revealed FC6-HC5 and FC6-HC6 to also form reversed micelles with aqueous core aspect ratios larger than 5, even at a low surfactant concentration of 16.7 mM and a relative high W_0 value of 20. To examine the formation of longer rod-like micelles at high surfactant concentrations, SANS measurements were performed with 35 mM or 50 mM FC6-HC*n*/D_2O/CO_2 mixtures at W_0 = 10, 45 ºC and 350 bar. These SANS profiles are presented in **Figure 4**.

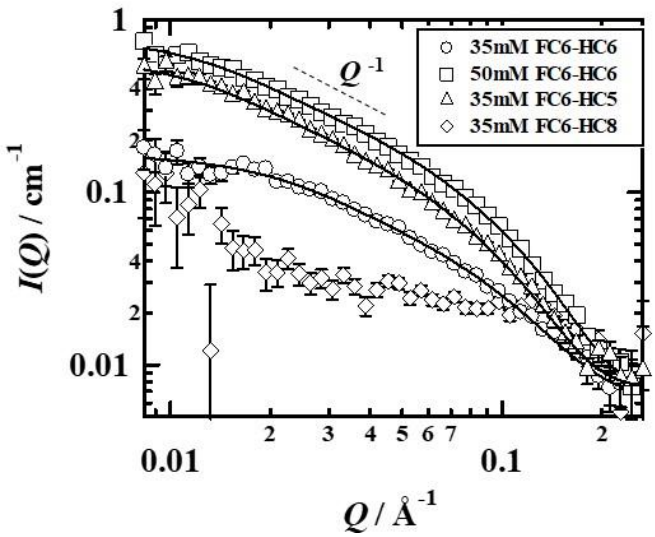

Figure 4. SANS profiles for 35 mM and 50 mM FC6-HC*n* (*n* = 5, 6 or 8)/D_2O/CO_2 mixtures with W_0 = 10 at 45 ºC and 350 bar (CO_2 density = 0.92 g/cm^3). Fitted curves were based on a model incorporating a Schultz distribution of cylindrical particles (polydisperse).

The poor solubility of FC6-HC8 in scCO_2 gave a turbid two-phase system and noisy SANS profiles. However, the shorter HC-tails of $n \leq 6$ allowed for the formation of one-phase W/CO_2 µEs in spite of high surfactant concentrations of 35 mM and 50mM. These systems display distinct SANS profiles with scaling as ~Q^{-1} over the intermediate Q-range, suggesting the formation of rod-like reversed micelles

[29,35,44,45]. To estimate radius/length for rod-like reversed micelles, Guinier plots of Ln [$I(Q)\ Q$] *vs* Q^2 and Ln [$I(Q)\ Q$] vs Q^2 were prepared (**Figure S4**). The SANS profiles were also analysed by fitting with theoretical curves of a cylinder particle model. Rod length and radius obtained by Guinier analysis were once again employed as a starting point for the curve fitting.

Table 3 Radii, lengths, aspect ratios ($X_{micelle}$ and X_{core}), intrinsic viscosity [η] and specific viscosity η_{sp} for rod-like reversed micelles and cores in FC6-HC*n*/D_2O/CO_2 mixtures with W_0=10 at 45 ºC and 350 bar.

n	[FC6-HCn] / mM	Guinier			Curve fitting		Aspect ratio		Viscosity	
		R_g /Å	L_{gui} / Å	R_{gui} /Å	L_{cyl} / Å	R_{cyl} / Å	X_{core}	X_{shell}	[η]	η_{sp}
5	35	70.1	243	20.8	879	12.2	36.0	17.7	30.9	2.07
6	35	30.4	105	31.4	166	12.0	7.0	3.8	4.4	0.24
	50	66.5	230	22.1	583	10.8	26.9	12.6	18.9	1.28
8	35	34.4	119	30.6	—	—	—	—		—

R_g, L_{gui} and R_{gui} are radius of gyration, rod length and rod radius respectively as obtained from the slopes of Guinier plots. L_{cyl} and R_{cyl} are cylinder length and radius when the experimental data were fitted by theoretical curve to a cylindrical particle model. Aspect ratios of core (X_{core}) and shell (X_{shell}) are calculated as $L_{cyl}/(2R_{cyl})$ and $(L_{cyl}+2l_{tail})/\{2(R_{cyl}+l_{tail})\}$, respectively. The surfactant tail length l_{tail} is identified as 13.4 Å from the perfluorohexyl phenyl tail length [35]. Intrinsic viscosity [η] and specific viscosity η_{sp} were calculated from equations (4) and (7), respectively.

Table 3 shows lengths, radii and aspect ratios of D_2O cores in rod-like reversed micelles given by Guinier and curve fitting analyses. Focusing on the core radius obtained from curve fitting, the radii at W_0 = 10 were almost constant at 10.8-12.2 Å, independent of concentration and HC-tail length of FC6-HC*n*. On the other hand, the length of FC6-HC6 reversed micelles increased by 3.5 times (166 Å → 583 Å)

when increasing surfactant concentration from 35 mM to 50 mM. When comparing FC6-HC5 and FC6-HC6 reversed micelles at 35 mM, FC6-HC5 formed rod-like reversed micelles 5.3 times longer than that of FC6-HC6. The longest rod-like reversed micelles in a W/CO_2 system previously reported was formed with the double-fluorinated tail surfactant with Ni^{2+} counterion, Ni(di-CF4)$_2$, with the length reaching 600 Å at a surfactant concentration of 50 mM with W_0 = 5 at 25 ºC and 400 bar [21,22]. Interestingly, the core length of FC6-HC5 reversed micelles has surpassed this value with the length reaching an unprecedented value of ~880 Å which is the new longest rod length ever reported in a W/CO_2 microemulsion.

In general, the viscosities of colloidal dispersions depend on particle concentration, shape and effective volume. Even in the case of rod-like reversed micelle/scCO_2 systems, a clear relationship between viscosity and aspect ratios of reversed micelles is apparent, and this is described in the supplementary data (**Figure S5**). To normalize for concentration, it is helpful to evaluate an intrinsic viscosity [η] at infinite dilution. To estimate the CO_2-thickening ability of the FC6-HC5 reversed micelles, [η] and viscosity of reversed micelle/CO_2 solutions were approximated as described below [21,49]. The [η] value is very sensitive to particle shape, for hard spheres [η] = 2.5, whereas for one-dimensional, anisotropic particles [η] is greater than this and can be approximated using equation (3) [50,51]:

$$[\eta] = 2.5 + 0.4075\,(X_{\text{micelle}} - 1)^{1.508} \qquad (3)$$

where X_{micelle} is the aspect ratio of the reversed micelle in **Table 3**. The [η] value can be used to estimate η_{sp} based on the structural parameters derived from SANS analysis and the known volume fraction ϕ_{p}. As such, equation (4) details an approximate formula which is valid for the dilute regime of $\phi_{\text{p}} < 0.2$, and the calculated viscosity has been confirmed to be coincident with the experimental data [52].

$$\eta_{\text{sp}} = [\eta]\,\phi_{\text{p}} + K_{\text{H}}\,[\eta]^2\,\phi_{\text{p}}^2 \qquad (4)$$

where the K_{H} is the Huggins coefficient for rods (in this case ~0.4) [51], calculated from and estimated shear rate and rotational diffusion coefficient D_{rot}; shear rate being obtained by analytical solution of the Navier–Stokes equation and D_{rot} being calculated using the SANS structural parameters and neat solution viscosity. The values ϕ_{p} can be calculated by following equation.

$$\phi_{\text{p}} = C_{\text{micelle}}\,V_{\text{micelle}} \qquad (5)$$

where $V_{micelle}$ and $C_{micelle}$ are molar volume and molar concentration of micelle, respectively. Those are obtained by equations (6) and (7) [29,35,53].

$$V_{micelle} = v_{micelle} N_A = \pi (R_{cyl} + l_{tail})^2 (L_{cyl} + l_{tail}) N_A \qquad (6)$$

$$C_{micelle} = (V_{D2O} C_{D2O} + V_{head} C_{surf})/(V_{core}) = C_{surf} (V_{D2O} W_0 + v_{head} N_A)/(v_{core} N_A) \qquad (7)$$

where $v_{micelle}$ is particle volume of micelle, l_{tail} is surfactant tail length (identified as 13.4 Å for FC6-HC*n* series from the perfluorohexyl phenyl part [35]), N_A is Avogadro's number, C_{surf} and C_{D2O}, $C_{micelle}$ are molar concentrations of surfactant, D_2O and reversed micelle, V_{D2O}, V_{head}, and V_{core} are molar volumes of D_2O, surfactant headgroup and D_2O core, v_{core} and v_{head} are volumes per D_2O core ($V_{core} = v_{core} N_A$) and headgroup ($V_{head} = v_{head} N_A$), respectively. The v_{core} values were calculated using radii and lengths obtained by the curve fitting, and the v_{head} values were referred from **Table 2**.

Table 3 also shows the viscosities, $[\eta]$ and η_{sp}, of the FC6-HC*n* rod-like reversed micelle/CO_2 solutions calculated from the equations (3) and (4), respectively. The viscosities at 35 mM were $[\eta] = 30.9$ and $\eta_{sp} = 2.07$ for the FC6-HC5 rod-like reversed micelles with the longest length $L_{cyl} = 879$ Å. These values are larger by 7.0 and 8.6 times respectively than for the FC6-HC6 micelles. An earlier paper [34] reported the largest viscosity enhancement of $\eta_{sp} = 1.0$ for the 75 mM Na-F7H4/W/CO_2 systems with $W_0 = 12.5$. However, the η_{sp} value of the FC6-HC5/W/CO_2 system now achieves and even greater viscosity enhancement.

3.3 Change in CPP, aggregation number, elongation of FC6-HC*n* reversed micelles with increasing surfactant concentration

The results in Sec 3.1-3.2 suggest the optimal HC-tail lengths to solubilize water and to form rod-like reversed micelles in $scCO_2$ is where n = 4 and 5, respectively. Why do these specific HC-tail lengths drive the water solubilization and the elongation of reversed micelles? A key to resolving this question may be in characteristics special to hybrid surfactants. For example, HC-tails in self-assembled hybrid surfactants may line up in the direction towards the reversed micelle centre (i.e. aqueous core) or the shell (i.e. CO_2-phase).

To investigate the HC-tail arrangement using aggregation properties of FC6-HC*n* (n = 4, 5, 6) in $scCO_2$, the aggregation number of surfactant per reversed micelle (N_{agg}) and occupied area per surfactant molecule at the W/CO_2 µE surface ($A_{C/W}$) were calculated by following equations.

$$N_{agg} = C_{surf}/C_{micelle} \qquad (8)$$

$$A_{C/W} = s_{core}/N_{agg} \qquad (9)$$

According to critical packing parameter (CPP) theory [37], CPP can be also obtained by

$$\mathrm{CPP} = v_{tail}/(A_{C/W}\, l_{tail}) \qquad (10)$$

where v_{tail} and l_{tail} are hydrophobic tail volume and length, respectively. According to this approach reversed micelles would be formed for surfactants with CPP > 1 (reversed cones form if the double-tail orients upward) to ~1 (cylindrical). If the hydrophobic part is assumed to be a truncated core, the volume should be [29,35,53]

$$v_{tail} = l_{tail}\{A_{C/W} + A_{tail} + (A_{C/W}\, A_{tail})^{0.5}\}/3 \qquad (11)$$

where A_{tail} is area per hydrophobic tail terminus, respectively. Then eq.(10) can be simply expressed as

$$\mathrm{CPP} = \{s_{micelle} + s_{core} + (s_{micelle}\, s_{core})^{0.5}\}/(3s_{core}) \qquad (12)$$

where $s_{micelle}$ is the surface area per reversed micelle [29,35,53]. In this study, the values of $s_{micelle}$ were calculated from the shape parameters ($R_{f\text{-}ell,a}$, $R_{f\text{-}ell,b}$, $R_{f\text{-}cyl}$, and $L_{f\text{-}cyl}$) and surfactant tail length l_{tail} assumed to be 13.4 Å (the length between the terminal F-atom and the C-atom bearing the sulfonate group [35]). The calculated aggregation properties N_{agg}, $A_{C/W}$, and CPP are listed in **Table S2** (supplementary data).

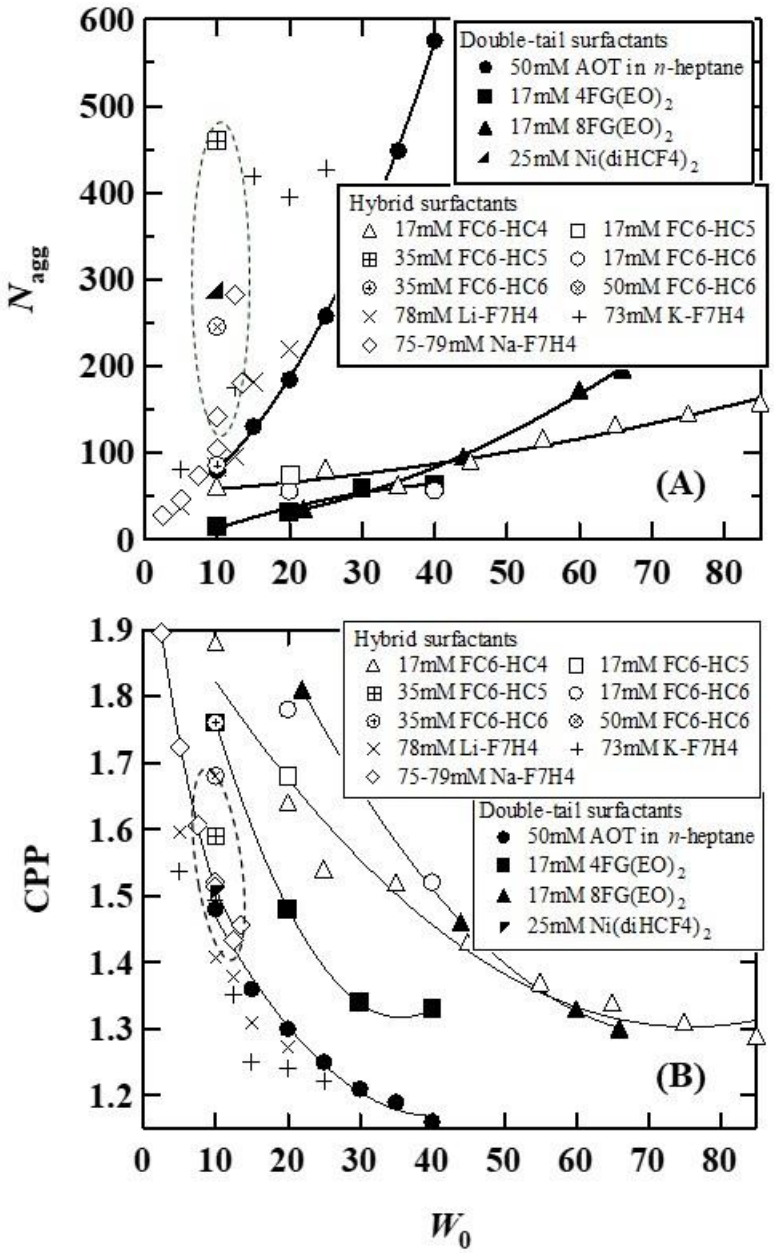

Figure 5. Changes in (A) aggregation number N_{agg} of reversed micelles and (B) critical packing parameter CPP as a function of W_0 for D_2O/CO_2 μEs with hybrid and double-tail surfactants or D_2O/*n*-heptane μEs with AOT. Experimental conditions were 45 °C and 350 bar for 17mM FC6-HC*n* (*n* = 4-6) and 17mM *n*FG(EO)$_2$ (*n* = 4, 8), 23-40 ºC and 380-400 bar for 78 mM Li-F7H4 and 73 mM K-F7H4, 75-79 mM Na-F7H4, 25 ºC and 350-400 bar for 25 mM Ni(di-HCF4)$_2$ in D_2O/CO_2 μEs, and 25 °C and 1 bar for 50 mM AOT in D_2O/*n*-heptane μEs.

Figures 5 shows changes in N_{agg} and CPP of FC6-HC*n* reversed micelles as a function of W_0 for FC6-HC*n*/D_2O/CO_2 mixtures at 45 ºC and 350 bar, based on the data in **Table S2**. The figures also include data for W/CO_2 µEs with the hybrid surfactant M-F7H4 (M=Li, K, Na) [3,33,34], double-tail surfactants *n*FG(EO)$_2$ (*n* = 4 and 8) [29], Ni(di-HCF4)$_2$ [21,22], and W/*n*-heptane with AOT [54]. Broken circles indicate conditions at which long rod-like reversed micelles with length > 250 Å formed.

Similar to other reversed micellar systems of AOT, M-F7H4 and *n*FG(EO)$_2$, FC6-HC*n* reversed micelles also exhibited the larger N_{agg} values at higher surfactant concentrations and W_0 values. The effect of W_0 was identified as the weaker contribution as N_{agg} for FC6-HC4 doubled when W_0 increased from 25 to 85. The effect of surfactant concentration is more pronounced, and N_{agg} was 74 at 17mM FC6-HC5 and W_0=20, but increased to 460 (i.e. 6.2 times larger) at 35 mM with almost same water content. The effects of water and surfactant concentrations on N_{agg} were based on swelling and elongating behavior of reversed micelles, respectively. The former increases µE droplet size with increasing $A_{W/C}$, whereas the latter increases rod-like reversed micelle length without an increase in $A_{W/C}$ as the relationships between $A_{W/C}$ and W_0 or surfactant concentration were clarified in supplementary data (**Figure S6**). The N_{agg} values in each *n*FG(EO)$_2$ and FC6-HC*n* series were similar at 17mM even if tail lengths *n* were different, suggesting that tail lengths of hybrid and double-tail surfactants have a small effect on N_{agg} at such a low surfactant concentration. However, the difference in N_{agg} became larger at higher surfactant concentration where morphology goes toward rod-like aggregates, even if the tail length is increased by just one methylene unit (i.e. N_{agg} = 460 for FC6-HC5 or 85 for FC6-HC6 at 35 mM). This would result from changes in CPP and/or hydrophilic-CO_2-philic balance (HCB) affecting differential Gibbs free energy (ΔG) [36-38,55] between the endcap and cylindrical body of rod-like reversed micelles, suggesting FC6-HC5 to have a larger ΔG (i.e. preferring the cylinder body rather than the cap).

From **Figure 5 (B)**, CPPs of all the surfactants were found to decrease with increasing W_0. This decreasing CPP trend was smallest for FC6-HC4 which has the highest W_0^{max}. This may be one of the reasons for its ability to solubilizing a large amount of water, as it can keep W/CO_2 interfacial curvature

as negative as possible, and the W/CO_2 µE is stable against increasing W_0. On the other hand, FC6-HC4 and *n*FG(EO)$_2$ are spherical W/CO_2 µEs and under the dilute condition they interestingly exhibited similar CPP values of ~1.3 when W_0 reached each the maximum solubilizing power (W_0^{max} = 45, 62 and 80 for 4FG(EO)$_2$, 8FG(EO)$_2$ and FC6-HC4 respectively [25,29,35]). The CPP of ~1.3 is suggested to be a common lowest limit to obtain spherical W/CO_2 µEs having the W_0^{max} values. However elongated micelles of M-F7H4 (M = Li and K) at near W_0^{max} appeared with the smaller CPP of < 1.3. Comparing between AOT/W/*n*-heptane and surfactant/W/CO_2 µEs at high surfactant concentrations ≥ 25mM, there were no significant difference in CPP. This implies no clear solvent effect between *n*-heptane and scCO_2 on CPP-W_0 (water-solubilization behaviour) for reversed-type µEs.

Long rod-like reversed micelles (broken circle) appeared at W_0 values of ~10, surfactant concentrations of ≥ 25 mM and 1.4 < CPP < 1.7. Surfactant concentration and CPP are well-known to affect reversed micelle morphology, and the appropriate values of CPP and the concentration seem reasonable based on aggregation behaviour in earlier surfactant/W/O systems [56]. Even if the concentration and W_0 values were appropriate for rod-like reversed micelles, surfactant/W/CO_2 systems not having the acceptable CPPs mentioned above (1.4 < CPP < 1.7) generated oblate ellipsoidal micelles (short rods) (examples include 35mM FC6-HC6, 78 mM Li-F7H4 [34] and 73 mM K-F7H4 [34]). The appropriate W_0 values for elongated micelle formation have rarely been discussed before. The addition of small amounts of water was reported to stabilise reversed micelles, and W_0 values of ~10 probably are enough to fully conduct attractive interactions between surfactant molecules arranged side by side in parallel to the rod-like reversed micelle axis. This can lower Gibbs energy of the cylindrical body compared with that of the endcap [36-38,55], and then induce a long rod morphology. However, increasing W_0 over 10 is likely to weaken the intermolecular attractive interactions due to the increased intermolecular distance [29,35,53], and this decreases the energy difference between the endcap and body of reversed micelles. This would in turn cause fragmentation of the rod-like reversed micelles.

Why did FC6-HC5 form the longest rod-like reversed micelles in the FC6-HC*n* series? This is a very interesting question and finding an answer will give an important insight in developing the next-

generation molecular designs for CO_2-philic rod-like reversed micelles as CO_2 thickeners. **Figure S6** demonstrates longer HC lengths generate larger $A_{C/W}$ resulting in smaller CPP values. This is probably due to the HC-tail lying on the interface as shown in **Figure S3**, and the CO_2-phobicity and hydrophobicity of HC-tails may be important feature which allows them to align on the micellar surface. Based on this, FC6-HC5 is suggested to have the optimal HC length to generate appropriate CPPs of ~1.6 for the longest rod-like reversed micelles. Therefore, the CO_2-phobic and hydrophobic HC-branch is identified as an important feature for rod-like reversed micelle formation, in addition to both CO_2-philic tail and hydrophilic groups as surfactant component parts. This is interesting new insight, since straight HC-chains were previously believed to be unsuccessful for stabilizing W/CO_2 microemulsions. However, it is now apparent that incorporating a HC-branch in CO_2-philic surfactant structure is a useful design feature.

4. Conclusions

Reversed micelles in $scCO_2$ can be considered VOC-free and energy-saving solvent systems for applications such as extraction, dyeing, dry cleaning, metal-plating, and organic/inorganic or nanomaterial synthesis [2]. These dispersions are even more promising, if the reversed micelles formed are rod-like assemblies, thus increasing CO_2 viscosity and significantly improving the currently poor sweep efficiency of EOR CO_2-flooding [3].

For applications such µEs should ideally be prepared with low levels of surfactant, be inexpensive and environmentally-benign. Therefore, finding low F-content surfactants which generate a high water solubilizing power and/or form long rod-like reversed micelles is key to designing useful CO_2-philic surfactants. Previous studies [35] found hybrid surfactants HC6-HC4 and FC6-HC5 were able to generate high solubilizing power and also rod-like micelles in $scCO_2$, respectively. To evaluate the effectiveness of each F-atom in the solubilization the solubilizing power (i.e. W_0 value per F-atom in the molecule) is 6.2 for FC6-HC4. This is 1.5 times larger than the most effective FC-surfactant in earlier papers [10-35]. The highest effectiveness per F-atom generated by hybrid structures is also an interesting concept for designing new CO_2-philic surfactants.

To find design criteria for practical CO_2-philic surfactants having less F-atoms, this study characterised in detail nanostructures of FC6-HC*n* aggregates in W/CO_2 mixtures by small-angle neutron scattering, to obtain area per headgroup, aggregation number, critical packing parameter by analysis and model fitting the SANS data. Detailed analysis about surfactant structure-aggregate morphology correlations suggested why FC6-HC4 and FC6-HC5 generated the highest solubilizing power and the longest rod-like reversed micelles in $scCO_2$, respectively. New findings and design criteria obtained in this study were described as followings (I)-(IV).

(I) At the dilute condition of 17mM, FC6-HC4/W/CO_2 µEs were identified to be ellipsoidal with high W_0 values > 20. The aqueous core radii increased with W_0 as a linear function and reached 39.1 Å and 77.8

Å at W_0 = 85 (≈ the maximum solubilizing power), being the largest core in spherical W/CO_2 µEs ever reported [10-35].

(II) FC6-HC5 formed rod-like reversed micelles 5.3 times longer than that of FC6-HC6 under the same conditions. The core length in FC6-HC5 reversed micelles was estimated as ~880 Å, and the length and aspect ratio were identified as the longest in W/CO_2 µEs studies. Estimated specific viscosity of the FC6-HC5 rod-like reversed micelle/CO_2 solution reached 2.07 (i.e. relative viscosity = 3.07), an increase of 8.6 times compared to FC6-HC5 micelles. Such a high (estimated) specific viscosity for FC6-HC5 was the largest viscosity enhancement of CO_2 compared to earlier surfactant/W/CO_2 systems [4-35].

(III) The critical packing parameter in spherical W/CO_2 µEs decreased with water loading into the reversed micelle cores, and finally reached the lowest values of ~1.3 (namely, the lowest limit in CPP for the spherical W/CO_2 µEs) at W_0 of each solubilizing power under the dilute surfactant condition of 17 mM. The decrease in CPP with increasing W_0 was the most moderate for FC6-HC4 allowing FC6-HC4 to achieve the highest solubilizing power.

(IV) Rod-like reversed micelles with lengths > 250 Å tended to appear at W_0 values of ~10, surfactant concentrations ≥ 25 mM and CPPs of 1.4-1.7. CPP for FC6-HC*n* was found to decrease with the longer HC length *n* and the larger $A_{C/W}$. The surfactant FC6-HC5 oriented into the rod-like reversed micelle formation is expected to have an optimal HC length for the appropriate CPP. Based on this consideration, the CO_2-phobic and hydrophobic HC-branch was identified as an important component of the surfactant to help induce rod-like reversed micelle formation.

As such these high water content W/CO_2 µEs and long rod-like reversed micelles could offer a new generation of universal solvents with unique properties. This study successfully identified a super-efficient W/CO_2-type solubilizer FC6-HC4 and the rod-like reversed micelle-forming surfactant FC6-HC5. These surfactants represent the most successful cases of low fluorine content additives and hence may make further impact in this field.

Acknowledgements

This project was supported by JSPS [KAKENHI, Grant-in-Aid for Scientific Research (B), No. 26289345, Fund for the Promotion of Joint International Research (Fostering Joint International Research) No. 15KK0221, Grant-in-Aid for Challenging Research (Exploratory), No.17K19002], and Leading Research Organizations (RCUK [through EPSRC EP/I018301/1], ANR [13-G8ME-0003]) under the G8 Research Councils Initiative for Multilateral Research Funding –G8-2012. CJ thanks the Japan Society for the Promotion of Science (JSPS) for an 18-month fellowship (The JSPS Postdoctoral Fellowship for Foreign Researchers) and EPSRC (grants EP/I018301 and EP/I018212/1). We also acknowledge STFC for the allocation of beam time, travel, and consumables grants at ISIS, and Dr. Kondo and Prof. Yoshino at Tokyo University of Science for providing hybrid surfactants FC6-HC*n*.

Appendix A. Supplementary data

Supplementary data associated with this article can be found, in the online version at.

References

[1] E.J. Beckman, Supercritical and near-critical CO_2 in green chemical synthesis and processing, J. Supercrit. Fluids 28 (2004) 121-191.

[2] E.L.V. Goetheer, M.A.G. Vortaman, J.T.F. Keurentjes, Opportunities for process intensification using reverse micelles in liquid and supercritical carbon dioxide, Chem. Eng. Sci. 54 (**1999**) 1589-1596.

[3] S. Cummings, R. Enick, S. Rogers, R. Heenan, J. Eastoe, Amphiphiles for supercritical CO_2, Biochimie 94 (2012) 94-100.

[4] K.A. Consani, R.D. Smith, Observations on the solubility of surfactants and related molecules in carbon dioxide at 50 ºC, J. Supercrit. Fluids 3 (1990) 51-65.

[5] W. Ryoo, S.E. Webber, K.P. Johnston, Water-in-carbon dioxide microemulsions with methylated branched hydrocarbon surfactants, Ind. Eng. Chem. Res. 42 (2003) 6348-6358.

[6] H. Lee, J.W. Pack, W. Wang, K.J. Thurecht, S.M. Howdle, Synthesis and phase behavior of CO_2-soluble hydrocarbon copolymer: poly(Vinyl Acetate-*alt*-Dibutyl Maleate), Macromolecules 43 (2010) 2276-2282.

[7] M. Sagisaka, K. Kudo, S. Nagoya, A. Yoshizawa, Highly methyl-branched hydrocarbon surfactant as a CO_2-philic solubilizer for water/supercritical CO_2 microemulsion, J. Oleo Sci. 62 (2013) 481-488.

[8] J. Eastoe, A. Mohamed, K. Trickett, S.Y. Chin, S. Cummings, M. Sagisaka, L. Hudson, S. Nave, R. Dyer, S. Rogers, R. Heenan, A universal surfactant for water, oils and CO_2, Langmuir 26 (2010) 13861–13866.

[9] M. Zulauf, H.F. Eicke, Inverted micelles and microemulsions in the ternary system water/aerosol-OT/isooctane as studied by photon correlation spectroscopy, J. Phys. Chem. 83 (1979) 480–486.

[10] C.T. Jr. Lee, P.A. Psathas, K.P. Johnston, J. deGrazia, T.W. Randolph, Water-in-carbon dioxide emulsions: formation and stability, Langmuir 15 (1999) 6781-6791.

[11] K.P. Johnston, K.L. Harrison, M.J. Klarke, S.M. Howdle, M.P. Heitz, F.V. Bright, C. Carlier, T.W. Randolph, Water-in-carbon dioxide microemulsions: a new environment for hydrophiles including proteins, Science 271 (1996) 624-626.

[12] R.G. Zielinski, S.R. Kline, E.W. Kaler, N.A. Rosov, Small-angle neutron scattering study of water in carbon dioxide microemulsions, Langmuir 13 (1997) 3934-3937.

[13] E.D. Niemeyer, F.V. Bright, The pH within PFPE reverse micelles formed in supercritical CO_2, J. Phys. Chem. B 102 (1998) 1474-1478.

[14] V.H. Dalvi, V. Srinivasan, P.J. Rossky, Understanding the effectiveness of fluorocarbon ligands in dispersing nanoparticles in supercritical carbon dioxide, J. Phys. Chem. C 114 (2010) 15553-15561.

[15] V.H. Dalvi, V. Srinivasan, P.J. Rossky, Understanding the relative effectiveness of alkanethiol ligands in dispersing nanoparticles in supercritical carbon dioxide and ethane, J. Phys. Chem. C 114 (2010) 15562-15573.

[16] X. Li, J. Turánek, P. Knötigová, H. Kudláčková, J. Mašek, S. Parkin, S.E. Rankin, B.L. Knutson, H.-J. Lehmler, *Colloid Surf. B* 73 (2009) 65-74.

[17] J. Eastoe, B.M.H. Cazelles, D.C. Steytler, J.D. Holmes, A.R. Pitt, T.J. Wear, R.K. Heenan, Water-in-CO_2 microemulsions studied by small-angle neutron scattering, Langmuir 13 (1997) 6980-6984.

[18] X. Dong, C. Erkey, H.-J. Dai, H.-C. Li, H.K. Cochran, J.S. Lin, Phase behavior and micelle size of an aqueous microdispersion in supercritical CO_2 with a novel surfactant, Ind. Eng. Chem. Res. 41 (2002) 1038-1042.

[19] J. Eastoe, A. Downer, A. Paul, D.C. Steytler, E. Rumsey, J. Penfold, R.K. Heenan, Fluoro-surfactants at air/water and water/CO_2 interfaces, Phys. Chem. Chem. Phys. 2 (2000) 5235-5242.

[20] J. Eastoe, A. Paul, A. Downer, D.C. Steytler, E. Rumsey, Effects of fluorocarbon surfactant chain structure on stability of water-in-carbon dioxide microemulsions. Links between aqueous surface tension and microemulsion, Langmuir 18 (2002) 3014-3017.

[21] K. Trickett, D. Xing, R. Enick, J. Eastoe, M.J. Hollamby, K.J. Mutch, S.E. Rogers, R.K. Heenan, D.C. Steytler, Rod-like micelles thicken CO_2, Langmuir 26 (2010) 83-88.

[22] S. Cummings, K. Trickett, R. Enick, J. Eastoe, CO_2: a wild solvent, tamed, Phys. Chem. Chem. Phys. 13 (2011) 1245-1696.

[23] D.C. Steytler, E. Rumsey, M. Thorpe, J. Eastoe, A. Paul, R.K. Heenan, Phosphate Surfactants for water-in-CO_2 microemulsions, Langmuir 17 (2001) 7948-7950.

[24] B. Xu, G.W. Lynn, J. Guo, Y.B. Melnichenko, G.D. Wignall, J.B. McClain, J.M. DeSimone, C.S. Johnston, Jr. NMR and SANS studies of aggregation and microemulsion formation by phosphorus fluorosurfactants in liquid and supercritical carbon dioxide, J. Phys. Chem. B 109 (2005) 10261-10269.

[25] M. Sagisaka, S. Iwama, A. Yoshizawa, A. Mohamed, S. Cummings, J. Eastoe, An effective and efficient surfactant for CO_2 having only short fluorocarbon chains, Langmuir 28 (2012) 10988-10996.

[26] M. Sagisaka, S. Yoda, Y. Takebayashi, K. Otake, B. Kitiyanan, Y. Kondo, N. Yoshino, K. Takebayashi, H. Sakai, M. Abe, Preparation of a W/scCO_2 microemulsion using fluorinated surfactants, Langmuir, 19 (2003) 220-225.

[27] M. Sagisaka, S. Yoda, Y. Takebayashi, K. Otake, Y. Kondo, N. Yoshino, H. Sakai, M. Abe, Effects of CO_2-philic tail structure on phase behavior of fluorinated Aerosol-OT analogue surfactant/water/supercritical CO_2 systems, Langmuir, 19 (2003) 8161-8167.

[28] M. Sagisaka, D. Koike, S. Yoda, Y. Takebayashi, T. Furuya, A. Yoshizawa, H. Sakai, M. Abe, K. Otake, Optimum tail length of fluorinated double-tail anionic surfactant for water/supercritical CO_2 microemulsion formation, Langmuir 23 (2007) 8784-8788.

[29] M. Sagisaka, S. Iwama, S. Ono, A. Yoshizawa, A. Mohamed, S. Cummings, C. Yan, C. James, S.E. Rogers, R.K. Heenan, J. Eastoe, Nanostructures in water-in-CO_2 microemulsions stabilized by double-chain fluorocarbon solubilizers", Langmuir, 29 (2013) 7618−7628.

[30] A. Mohamed, M. Sagisaka, F. Guittard, S. Cummings, A. Paul, S.E. Rogers, R.K. Heenan, R. Dyer, J. Eastoe, Low fluorine content CO_2-philic surfactants. Langmuir 27 (2011) 10562-10569.

[31] A. Mohamed, T. Ardyani, M. Sagisaka, S. Ono, T. Narumi, M. Kubota, P. Brown, C. James, J. Eastoe, A. Kamari, N. Hashim, I.M. Isa, S.A. Bakar, Economical and efficient hybrid surfactant with low fluorine content for the stabilisation of water-in-CO_2 microemulsions, J. Supercrit. Fluids, 98 (2015) 127-136.

[32] K. Harrison, J. Goveas, K.P. Johnston, E.A. O'Rear III, Water-in-carbon dioxide microemulsions with a fluorocarbon-hydrocarbon hybrid surfactant, Langmuir 10 (1994) 3536-3541.

[33] A. Dupont, J. Eastoe, L. Martin, D.C. Steytler, R.K. Heenan, F. Guittard, E.T. Givenchy, Hybrid fluorocarbon-hydrocarbon CO_2-philic surfactants. 2. Formation and properties of water-in-CO_2 microemulsions, 20 (2004) 9960-9967.

[34] S. Cummings, D. Xing, R. Enick, S. Rogers, R. Heenan, I. Grillo, J. Eastoe, Design principles for supercritical CO_2 viscosifiers. Soft Matter 8 (2012) 7044–7055.

[35] M. Sagisaka, S. Ono, C. James, A. Yoshizawa, A. Mohamed, F. Guittard, S.E. Rogers, R.K. Heenan, C. Yan, J. Eastoe, Effect of fluorocarbon and hydrocarbon chain lengths in hybrid surfactants for supercritical CO_2, Langmuir 31 (2015) 7479-7487.

[36] S.R.P. da Rocha, K.L. Harrison, K.P. Johnston, Effect of surfactants on the interfacial tension and emulsion formation between water and carbon dioxide, Langmuir 15 (1999) 419–428.

[37] J.N. Israelachvili, Measurements of hydration forces between macroscopic surfaces, Chem. Scr. 25 (1985) 7-14.

[38] P.A. Winsor, Hydrotropy, solubilisation and related emulsification processes, Trans. Faraday. Soc. 54 (1948) 376-398.

[39] N. Yoshino, K. Hamano, Y. Omiya, Y. Kondo, A. Ito, M. Abe, Syntheses of hybrid anionic surfactants containing fluorocarbon and hydrocarbon chains, Langmuir 11 (1995) 466–469.

[40] A. Ito, H. Sakai, Y. Kondo, N. Yoshino, M. Abe, Micellar solution properties of fluorocarbon−hydrocarbon hybrid surfactants, Langmuir 12 (1996) 5768–5772.

[41] A. Dupont, J. Eastoe, M. Murray, L. Martin, F. Guittard, E.T. de Givenchy, R.K. Heenan, Hybrid fluorocarbon-hydrocarbon CO_2-philic surfactants. 1. Synthesis and properties of aqueous solutions, Langmuir 20 (2004) 9953-9959.

[42] Merck Index. 11th Edition. Merck & Company, Inc., Rahway, NJ; 1989.

[43] M. Kotlarchyk, S.-H. Chen, J.S. Huang, M.W. Kim, Structure of three-component. Microemulsions in the critical region determined by small angle neutron scattering data, Phys. Rev. A 29 (1984) 2054-2069.

[44] M. Sagisaka, S. Iwama, S. Hasegawa, A. Yoshizawa, A. Mohamed, S. Cummings, S. E. Rogers, R. K. Heenan, J. Eastoe, Super-efficient surfactant for stabilizing water-in-carbon dioxide microemulsions, Langmuir 27 (2011) 5772–5780.

[45] A. Guinuier, G. Fournet, Small-Angle Scattering of X-Rays, Wiley, New York, 1956.

[46] G. Porod, Die Röntgenkleinwinkelstreuung von dichtgepackten kolloiden Systemen. *Kolloid-Zeitschrift* 124 (195**1**) 83-114.

[47] M. Sagisaka, D. Koike, Y. Mashimo, S. Yoda, Y. Takebayashi, T. Furuya, A. Yoshizawa, H. Sakai, M. Abe, K. Otake, Water/supercritical CO_2 microemulsions with mixed surfactant systems, Langmuir 24 (2008) 10116–10122.

[48] W. Kunz, Specific ion effects in colloidal and biological systems, Curr. Opin. Colloid Interface Sci. 15 (2010) 34-39.

[49] J. Peach, A. Czajka, G. Hazell, C. Hill, A. Mohamed, J.C. Pegg, S.E. Rogers, J. Eastoe, Tuning micellar structures in supercritical CO_2 using surfactant and amphiphile mixtures, Langmuir 33 (2017) 2655-2663.

[50] D.H. Berry, W.B. Russel, The rheology of dilute suspensions of slender rods in weak flows, J. Fluid Mech. 180 (1987), 475-494.

[51] A.M. Wierenga, A.P. Philipse, Low-shear viscosity of isotropic dispersions of (Brownian) rods and fibres; a review of theory and experiments, Colloids Surf., A 137 (1998) 355−372.

[52] R. Simha, The influence of brownian movement on the viscosity of solutions, J. Phys. Chem. 44 (1940) 25-34.

[53] M. Sagisaka, S. Ogiwara, S. Ono, C. James, A. Yoshizawa, A. Mohamed, S.E. Rogers, R.K. Heenan, C. Yan, J.A. Peach, J. Eastoe, A new class of amphiphiles designed for use in water-in-supercritical CO_2 microemulsions, Langmuir 32 (2016) 12413–12422.

[54] S. Nave, J. Eastoe, R.K. Heenan, D. Steytler, I. Grillo, What is so special about Aerosol-OT? 2. Microemulsion systems, Langmuir 16 (2000) 8741-8748.

[55] S. Dhakal, R. Sureshkumar, Topology, length scales and energetics of surfactant micelles, J. Chem. Phys. 143 (2015) 024905.

[56] K. Trickett, J. Eastoe, Surfactant-based gels, Adv. Colloid Interface Sci. 144 (2008) 66-74.

Figure captions

Figure 1. SANS profiles for FC6-HC*n* (*n* = 4 or 6)/D_2O/CO_2 mixtures with different W_0 values at 45 ºC and 350 bar (CO_2 density = 0.92 g/cm^3). Fitted curves were based on a model incorporating a Schultz distribution of polydisperse ellipsoid particles. The molar ratio of the surfactant to CO_2 was fixed at 8×10^{-4} ([Surfactant] = ~16.7 mM at the experimental conditions).

Figure 2. Changes in ellipsoidal aqueous core radii $R_{\text{ell-a}}$ and $R_{\text{ell-b}}$ for the 16.7 mM FC6-HC*n*/D_2O/CO_2 μEs as a function of W_0 at 45 ºC and 350 bar. The data were taken from **Table S1**. Solid and broken lines show linear functions fitted with the data for FC6-HC4 and FC6-HC6, respectively.

Figure 3. Relationship between volume-to-surface area ratio ($v_{\text{core}}/s_{\text{core}}$) of aqueous cores and W_0 for the 17mM FC6-HC$_n$/D_2O/CO_2 μEs at 45 ºC and 350 bar. The $v_{\text{core}}/s_{\text{core}}$ values were calculated with ellipsoidal core radii listed in **Table S1**. The graph also displays data for D_2O/CO_2 μEs with 73 mM K-F7H4, 78 mM Li-F7H4, 75-79 mM Na-F7H4, 79 mM Na-F8H4 at 23-40 ºC and 380-400 bar reported in earlier papers [3,33,34].

Figure 4. SANS profiles for 35 mM and 50 mM FC6-HC*n* (*n* = 5, 6 or 8)/D_2O/CO_2 mixtures with W_0 = 10 at 45 ºC and 350 bar (CO_2 density = 0.92 g/cm^3). Fitted curves were based on a model incorporating a Schultz distribution of cylindrical particles (polydisperse).

Figure 5. Changes in (A) aggregation number N_{agg} of reversed micelles and (B) critical packing parameter CPP as a function of W_0 for D_2O/CO_2 μEs with hybrid and double-tail surfactants or D_2O/*n*-heptane μEs with AOT. Experimental conditions were 45 °C and 350 bar for 17mM FC6-HC*n* (*n* = 4-6) and 17mM *n*FG$(EO)_2$ (*n* = 4, 8), 23-40 ºC and 380-400 bar for 78 mM Li-F7H4 and 73 mM K-F7H4, 75-79 mM Na-F7H4, 25 ºC and 350-400 bar for 25 mM Ni(di-HCF4)$_2$ in D_2O/CO_2 μEs, and 25 °C and 1 bar for 50 mM AOT in D_2O/*n*-heptane μEs.